

KINEMATIC CALIBRATION OF 6R SERIAL MANIPULATORS USING RELATIVE MEASUREMENTS

Chao-Chia D. Lu, M. John D. Hayes.

Department of Aerospace and Mechanical Engineering, Carleton University, Ottawa, ON, Canada.

Email: chaochialu@email.carleton.ca; jhayes@mae.carleton.ca

ABSTRACT

In this paper, an approach to the kinematic calibration of serial manipulators with six revolute joints in general using relative position and orientation measurements is presented, and a Thermo CRS A465 is used for illustration. The definition of the errors used for the calibration process are first introduced, then the kinematic model that describes the manipulator pose (position and orientation) using the kinematic parameters is discussed. The pose of the manipulator is specified by six independent position and orientation parameters. The kinematic model presented is based on the nominal Denavit-Hartenburg (DH), along with the kinematic error model that describes the changes in the manipulator pose to the relative errors between the nominal and actual DH parameters. The results of two simulated measurements using the position and orientation are presented, and the performance of the kinematic error identification technique is discussed.

Keywords: kinematic calibration; 6R serial manipulator; singular value decomposition; relative position and orientation measurement.

CALIBRATIONS CINÉMATIQUE DU MANIPULATEUR SÉRIEL DE 6R UTILISANT DES MESURES RELATIVE

RÉSUMÉ

Dans ce papier, une approche à la calibration cinématique des manipulateurs sériels avec six couples rotatoires utilisant généralement des positions et mesures d'orientation générale est présentée, et un Thermo-CRS A465 est utilisé pour illustration. La définition des erreurs utilisées pour le processus de calibration sont d'abord introduites, puis le modèle cinématique qui décrit la pose du manipulateur (position et orientation) utilisant les paramètres cinématiques est discuté. La pose du manipulateur est spécifiée par six paramètres de positions et orientations indépendants. Le modèle cinématique présenté est basé sur la nominal Denavit-Hartenburg (DH), avec le modèle d'erreurs cinématiques qui décrit les changements de la pose du manipulateur aux erreurs relatives entre les paramètres DH nominal et actuel. Les résultats des deux mesures simulées utilisant les positions et orientations sont présentés, et la performance de la technique d'identification d'erreurs cinématiques est discutée.

Mots-clés : Calibration cinématique ; manipulateur sériel de 6R ; valeur seule de décomposition ; mesures de position et d'orientation relative.

1. INTRODUCTION

Robot manipulator calibration has been an active research topic for many years [1]. It is highly essential for robot manufacturing systems, because manipulators generally have vastly superior repeatability [2] compared to their accuracy, which can render them unfeasible for some applications. Mooring, Roth, and Driels discussed and summarized the details of the kinematic calibration steps and conducted examples regarding kinematic calibration of an industrial robot in [3]. The discrepancy between the accuracy and the repeatability, which typically is several orders of magnitude, is due mainly to the embedded nominal kinematic model in the controller [1, 3, 4]. It is evident that 95% of the measured errors are geometric errors, and the remaining 5% are from non-geometric errors [5]. This makes kinematic calibration the primary focus for research on accuracy enhancement.

Many researchers have addressed various issues in kinematic calibration procedures, whether it is in the area concerning the development of kinematic model [6–8], measurement systems [9–13], algorithms for parameter identification [14, 15], or compensating errors in the controller [3]. Absolute accuracy is difficult to measure due to the lack of a well-defined and mechanically accessible base coordinate frame for the manipulator. This coordinate reference frame is generally defined by the manufacturers to be inside the body of the arm, and it is difficult to measure coordinates with respect to it. The process of calibrating the transformation from the reference frame of the measurement system to the base frame can be expensive and time consuming. This process can be avoided by using relative position measurements instead. There have been several sets of results reported in [16–18].

In particular, Simpson and Hayes [16] first discussed the kinematic calibration of six-axis serial robots using the relative measurement concept. The work involves the development of a kinematic calibration procedure that uses relative position measurements along a precision ruled straight edge obtained using a tool-flange mounted camera [17]. The procedure requires the robot to move incremental distances along the ruler and uses image processing to estimate the geometric errors from differences in pairs of sequential images. The method requires the nominal DH parameters, which consists of 24 parameters to construct a 6R serial manipulator model. This method uses only the position measurements along a precision machined straight edge results in only 18 of 24 parameter errors being identified. In [18], In-Chul Ha presented a somewhat different relative position measurement concept. Ha's method models the manipulator kinematics using the modified DH parameters that takes into the account two consecutive parallel, or nearly parallel joint axes. The experimental setup described in this paper consists of a 6 DOF manipulator (MOTOMAN UP 20), a laser height sensor, a grid plate, and a PC.

The objective set out for the work presented herein is to develop a simple, low cost, kinematic calibration method that does not rely on absolute measurements which can identify the absolute errors in the robot kinematic model. It builds upon the work in [16, 17], which used only relative position measurements. In addition, the work presented in this paper uses relative orientation measurements to enhance the precision of the identified errors. Kinematic calibration is performed to improve the accuracy of the manipulator up to the limit of its repeatability. Most of the kinematic calibration systems reviewed require the *absolute* measurement of the end-effector pose, both position and orientation, which implies that the pose measurements are made with respect to a fixed coordinate reference frame. However, since robot tasks generally involves moving between either computed or taught poses, the implication is that comparing the geometric differences between commanded and achieved poses should reveal the geometric errors in the kinematic parameters of the nominal robot geometric model.

Consider an image of a chessboard viewed by a CCD camera mounted to a robot tool flange, as illustrated in Figure 1. If the robot is commanded to view the chessboard from a specified pose, the controller must compute the joint angles required to attain the pose, thereby relying on the robot accuracy. If the computed joint angles are stored and the robot is commanded to some other random pose, then to return

to the stored joint angles, the final pose will rely on the repeatability. The geometric differences between the corresponding images is a measure of the relative positioning and orienting errors, assuming a suitably calibrated camera. The relative error in the two images is illustrated in Figure 3. Note that even the relative measurement concepts in the existing literature, [16–18] for example, do not consider the orientation error, presumably because it is difficult and expensive to measure with high precision. However, we shall demonstrate that, at least conceptually, the relative measurement concept and kinematic model presented in this paper will enable the identification of the absolute position and orientation error so that it can be calibrated out, at least up to the limit of the repeatability of the robot mechanical system.

2. THE RELATIVE MEASUREMENT CONCEPT

The kinematic geometry of every robot manipulator is affected by errors resulting from machining tolerances. These errors manifest themselves as poor accuracy in tasks where robot poses are computed rather than taught. This is because the required joint angles are determined by solving the inverse kinematics problem using the nominal kinematic geometry, rather than simply returning to a taught pose whose joint angles are read from the joint encoders.

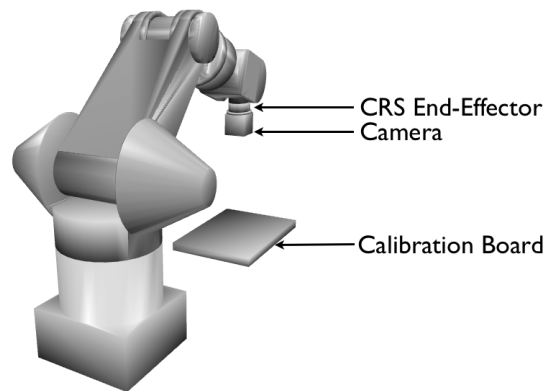


Fig. 1. Relative measurement setup for a Thermo CRS A465.

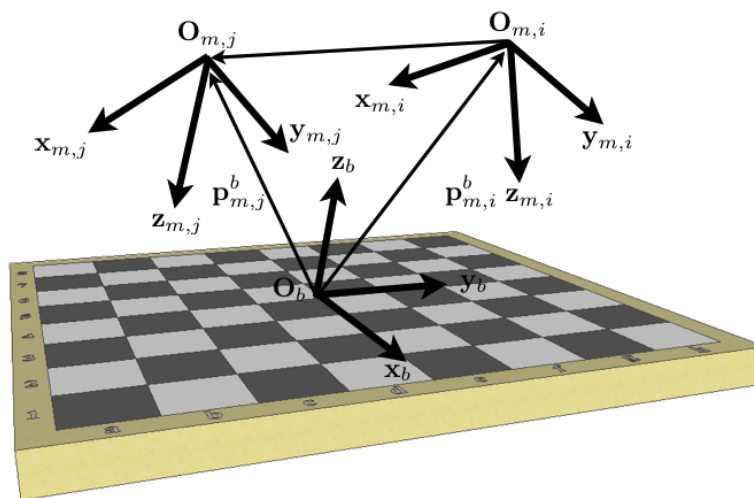


Fig. 2. Reference frames relative to the calibration board for the i^{th} and j^{th} poses.

The relative measurement concept applied to parameter identification involves comparing two sequential images of a registration object obtained with a robot-mounted camera. The errors in the kinematic model parameters are embedded in the deviation between the two images. Figure 1 is a conceptual illustration of the experimental setup. The measurements of the end-effector pose are made as the camera pose relative to a known reference frame on the calibration board. Figure 2 illustrates the geometry of the measurements

Consider a Thermo CRS A465 moving to commanded poses i and j . When the A465 settles in the i^{th} pose, an image of the chessboard registration object is taken, and the pose of the camera is extracted from the geometry of the image of the known chessboard. Another image after A465 settles in the j^{th} pose. The relative accuracy of the pose can be obtained from the difference between the i^{th} and the j^{th} configuration. In every commanded configuration of A465, there exists a pose based on the nominal model and the measured pose. The nominal model is embedded in the controller where the kinematic parameters are based on the designed dimensions. Figure 3 shows an exaggerated illustration of the relative errors between two poses observed from the vantage points of the nominal and actual kinematic geometry of the robot.

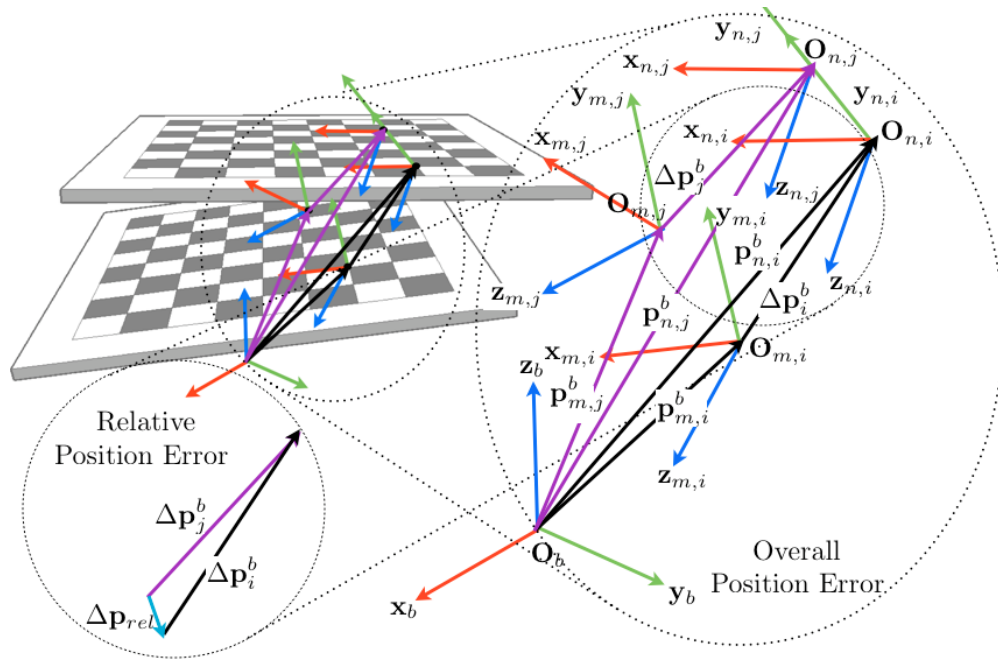


Fig. 3. Exaggerated relative pose errors.

The pose of the end-effector relative to the manipulator's base can be expressed as an array containing measures of both position and orientation

$$\mathbf{x}_e^b = \begin{bmatrix} \mathbf{p}_e^b \\ \Phi_e^b \end{bmatrix}. \quad (1)$$

The linear displacement, or position, components of the measured end-effector pose using the configurations i and j are the combination of the pose generated using the nominal kinematic geometry plus an additional component created by the geometric errors:

$$\mathbf{p}_{m,i}^b = \mathbf{p}_{n,i}^b + \Delta\mathbf{p}_i^b, \quad (2a)$$

$$\mathbf{p}_{m,j}^b = \mathbf{p}_{n,j}^b + \Delta\mathbf{p}_j^b. \quad (2b)$$

The relative position errors are described as the error of the deviations in the j^{th} configuration with respect to the deviations in the i^{th} configuration, and can be written, in terms of Eqs. (2a) and (2b), as

$$\Delta \mathbf{p}_{rel} = \Delta \mathbf{p}_j^b - \Delta \mathbf{p}_i^b = (\mathbf{p}_{m,j}^b - \mathbf{p}_{n,j}^b) - (\mathbf{p}_{m,i}^b - \mathbf{p}_{n,i}^b). \quad (3)$$

Figure 4 shows a simple illustration of rigid bodies with attached frames $\{1\}$ and $\{2\}$ rotated about the \mathbf{z} -axis relative to the base coordinate frames (Frame $\{b\}$) by angles of ψ_1 and ψ_2 . This rotation displaces the \mathbf{x} and \mathbf{y} axes of the attached frames by $\psi_{x,1}^b$, $\psi_{x,2}^b$ and $\psi_{y,1}^b$, $\psi_{y,2}^b$, respectively. The angle of the rotation of the attached frames can be expressed as

$$\psi_{x,2}^b = \psi_{x,1}^b + \psi_{x,2}^1, \quad \psi_{y,2}^b = \psi_{y,1}^b + \psi_{y,2}^1. \quad (4)$$

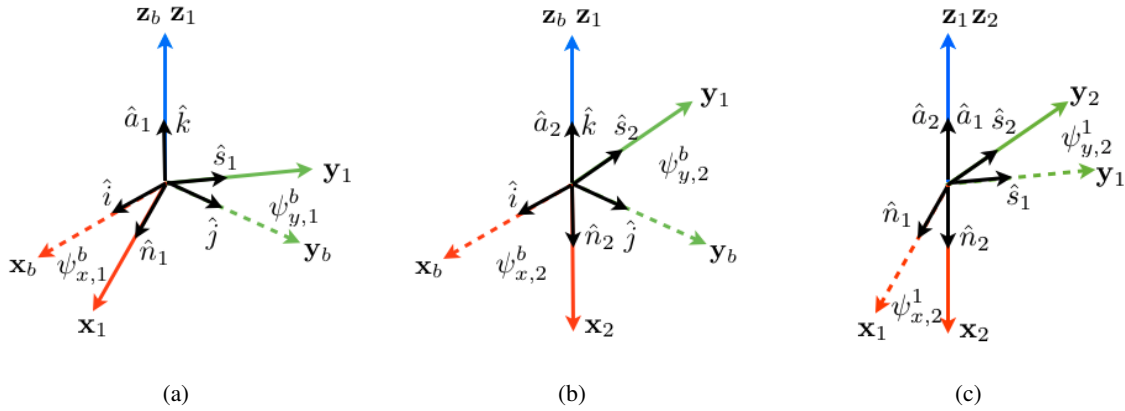


Fig. 4. Relative angular displacements.

Reconsidering Figure 3 again, the measured orientation of the manipulator, m , moving in the commanded configurations i and j can also be expressed in the same form as Eq. (2)

$$\Phi_{m,i}^b = \Phi_{n,i}^b + \Delta \Phi_i^b, \quad \Phi_{m,j}^b = \Phi_{n,j}^b + \Delta \Phi_j^b, \quad (5)$$

where $\Phi = [\hat{n}, \hat{s}, \hat{a}]^T$ defines the orientation of the \mathbf{x} , \mathbf{y} , and \mathbf{z} axes, respectively, of the coordinate frames of interest. Now, the relative orientation errors can be written as

$$\Delta \Phi_{rel} = \Delta \Phi_j^b - \Delta \Phi_i^b = (\Phi_{m,j}^b - \Phi_{n,j}^b) - (\Phi_{m,i}^b - \Phi_{n,i}^b). \quad (6)$$

The next step required for calibration is to construct a mathematical model that describes the pose of the end-effector, which can be represented as

$$\mathbf{x}_e^b = \mathbf{k}(\mathbf{q}), \quad (7)$$

where the parameter known as the joint variable array, \mathbf{q} , contains a measure of angle θ for revolute joint angles, or a measure of distance d for variable offsets in prismatic joints; the array \mathbf{x} contains three linearly independent position coordinates and three linearly independent orientations about the position coordinate axes of a coordinate reference frame attached to the end-effector, e , expressed in the relatively non-moving robot base coordinate reference frame, b ; while $\mathbf{k}(\cdot)$ is the nonlinear function defined using a set of kinematic parameters, that maps \mathbf{q} to \mathbf{x} . This kinematic model represents the forward kinematics model of the manipulator, and is embedded in the controller. The details of the kinematic parameters used in the model

are selected by the robot designers. In this work, the nominal Denavit-Hartenberg (DH) parameters [19] are used to model the spatial geometric relationships between sequential serial joints.

For typical applications, the only variable in Eq. (7) is the joint variable array \mathbf{q} . However, every kinematic parameter in Eq. (7) is treated as variable for kinematic calibration, because the purpose of the calibration process is to identify the errors in the designed nominal values. Using the DH parameters, Eq. (7) can be re-expressed as

$$\mathbf{x}_e^b = \mathbf{k}(\boldsymbol{\theta}, \mathbf{a}, \mathbf{d}, \boldsymbol{\alpha}), \quad (8)$$

where $\boldsymbol{\theta}$, \mathbf{a} , \mathbf{d} , and $\boldsymbol{\alpha}$ are the DH parameter arrays representing joint values, link lengths, link offsets, and joint twists, respectively [19]. The deviation between the specified pose and the actual pose, largely caused by the forward kinematic effects due to the DH parameter errors, is obtained from the measurement system and can be expressed as the deviations from the nominal parameters, such that

$$\mathbf{x}_m^b = \mathbf{x}_n^b + \Delta\mathbf{x}^b = \mathbf{k}(\boldsymbol{\theta}_n + \Delta\boldsymbol{\theta}, \mathbf{a}_n + \Delta\mathbf{a}, \mathbf{d}_n + \Delta\mathbf{d}, \boldsymbol{\alpha}_n + \Delta\boldsymbol{\alpha}). \quad (9)$$

The subscript n denotes the nominal fixed parameters that are equal to the design data of the mechanical structure, whereas the nominal joint angles are the recorded joint displacements during the measurements. Let $\Delta\boldsymbol{\zeta} = [\Delta\boldsymbol{\theta}, \Delta\mathbf{a}, \Delta\mathbf{d}, \Delta\boldsymbol{\alpha}]^T$ be the errors in the DH parameters. The errors in the controllable parameter can be thought of as bias errors, constant offsets from the prescribed values, which can be $\Delta\boldsymbol{\theta}_o$ or $\Delta\mathbf{d}_o$ depending on the controllable joint type. In this paper we will consider only revolute joints, however the concept applies equally to prismatic joints. Hence, the deviations in the remaining three parameters are fixed linear and angular displacements: $\Delta\mathbf{a}$; $\Delta\boldsymbol{\alpha}$; and $\Delta\mathbf{d}$.

The relative errors in the manipulator pose, $\Delta\mathbf{x}^b = \mathbf{x}_m^b - \mathbf{x}_n^b$, give a measure of accuracy at the given pose. Assuming that the deviations in the poses are small, the kinematic error can be found by evaluating the Taylor's series about the nominal DH parameters and considering only the first, linear terms.

$$\Delta\mathbf{x}^b = \frac{\partial\mathbf{k}}{\partial\boldsymbol{\theta}}\Delta\boldsymbol{\theta}_o + \frac{\partial\mathbf{k}}{\partial\mathbf{a}}\Delta\mathbf{a} + \frac{\partial\mathbf{k}}{\partial\mathbf{d}}\Delta\mathbf{d} + \frac{\partial\mathbf{k}}{\partial\boldsymbol{\alpha}}\Delta\boldsymbol{\alpha}. \quad (10)$$

This gives a linear approximation of the differential deviations of the DH parameters. Eq. (10) can then be rearranged into

$$\Delta\mathbf{x}^b = \frac{\partial\mathbf{k}}{\partial\boldsymbol{\zeta}}\Delta\boldsymbol{\zeta} = \mathbf{J}\Delta\boldsymbol{\zeta}, \quad (11)$$

where \mathbf{J} is a $M \times N$ identification Jacobian matrix in the form of $\mathbf{J} = [\mathbf{J}_\theta, \mathbf{J}_a, \mathbf{J}_d, \mathbf{J}_\alpha]$. The dimension M depends on the size of $\Delta\mathbf{x}^b$. If both the orientation and position are measured, then $M = 6n_p$, where there are three independent unit vectors describing the reference coordinate system basis directions (\hat{n} , \hat{s} , \hat{a}), and three coordinates for the origin of the associated coordinate system relative to a non-moving reference coordinate system, (p_x , p_y , p_z), and n_p is the number of poses. If only relative position measurements are made, then $M = 3n_p$. The dimension N depends on the number of kinematic parameters to be identified. The DH convention used in this paper consists of 4 parameters for each joint, and the manipulator is a 6R serial manipulator resulting in $N = 24$ parameters to be identified.

Using Eqs. (3) and (6), the kinematic error model for the relative measurement concept can be written as

$$\begin{aligned} \Delta\mathbf{x}_{rel} = & \left[\left(\frac{\partial\mathbf{k}}{\partial\boldsymbol{\theta}} \right)_j - \left(\frac{\partial\mathbf{k}}{\partial\boldsymbol{\theta}} \right)_i \right] \Delta\boldsymbol{\theta}_o + \left[\left(\frac{\partial\mathbf{k}}{\partial\mathbf{a}} \right)_j - \left(\frac{\partial\mathbf{k}}{\partial\mathbf{a}} \right)_i \right] \Delta\mathbf{a} + \\ & \left[\left(\frac{\partial\mathbf{k}}{\partial\mathbf{d}} \right)_j - \left(\frac{\partial\mathbf{k}}{\partial\mathbf{d}} \right)_i \right] \Delta\mathbf{d} + \left[\left(\frac{\partial\mathbf{k}}{\partial\boldsymbol{\alpha}} \right)_j - \left(\frac{\partial\mathbf{k}}{\partial\boldsymbol{\alpha}} \right)_i \right] \Delta\boldsymbol{\alpha}, \end{aligned} \quad (12)$$

which can be expressed in the same form as Eq. (11)

$$\Delta \mathbf{x}_{rel} = \mathbf{J}_{rel} \Delta \zeta, \quad (13)$$

where $\mathbf{J}_{rel} = \mathbf{J}_j^i = \mathbf{J}_j - \mathbf{J}_i$ is the identification Jacobian for relative measurement. Since the identification Jacobian is a non-square matrix, \mathbf{J}_{rel} is generally not invertible. An approximate solution for $\Delta \zeta$ in Eq. (13) can nonetheless be found by using a numerically robust application of the Moore-Penrose generalized inverse:

$$\Delta \zeta = (\mathbf{J}_{rel}^T \mathbf{J}_{rel})^{-1} \mathbf{J}_{rel}^T \Delta \mathbf{x}_{rel} = \mathbf{J}_{rel}^+ \Delta \mathbf{x}_{rel}. \quad (14)$$

A suitable number of pose measurements, n_p , is required to identify $\Delta \zeta$. In order to converge to an optimal result in the least-squares sense, Eq. (13) must be an overdetermined system where the number of linear equations ($3n_p$ or $6n_p$) must be suitably greater than the 24 unknown parameters.

3. SIMULATION

A flowchart summarizing a simulation of kinematic calibration using the relative measurement concept is presented in Figure 5. The input is the kinematic geometry of the manipulator being calibrated. A Thermo CRS A465 was selected for illustration, and its nominal DH parameters are listed in Table 1. The algorithm output consists of the identified DH parameter errors for the simulation.

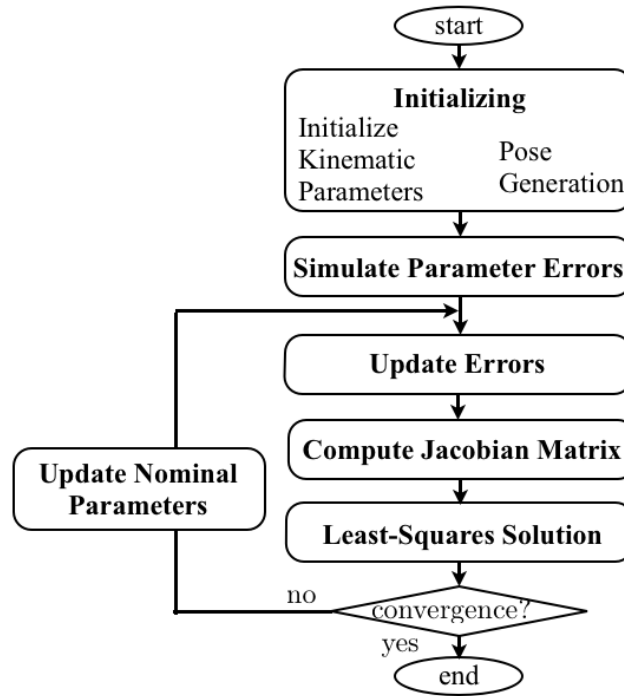


Fig. 5. Flowchart for the simulation of relative measurement concept.

The simulation begins with the synthesis of random errors for the DH parameters to mimic those of an actual manipulator. A trajectory in Cartesian space must then be selected for the end-effector. The inverse kinematics of the A465 are then computed to determine the trajectory in joint space. Figures 6(a) and 6(b) illustrate the Cartesian trajectory and the corresponding required joint space trajectory planned for this particular experiment, respectively.

| Joint Number, i | θ_i (degrees) | α_i (degrees) | a_i (m) | d_i (m) |
|-------------------|----------------------|----------------------|-----------|-----------|
| 1 | θ_1 | 90 | 0 | 0.33 |
| 2 | θ_2 | 0 | 0.303 | 0 |
| 3 | θ_3 | 90 | 0 | 0 |
| 4 | θ_4 | -90 | 0 | 0.33 |
| 5 | θ_5 | 90 | 0 | 0 |
| 6 | θ_6 | 0 | 0 | 0.076 |

Table 1. The nominal DH parameters for Thermo CRS A465.

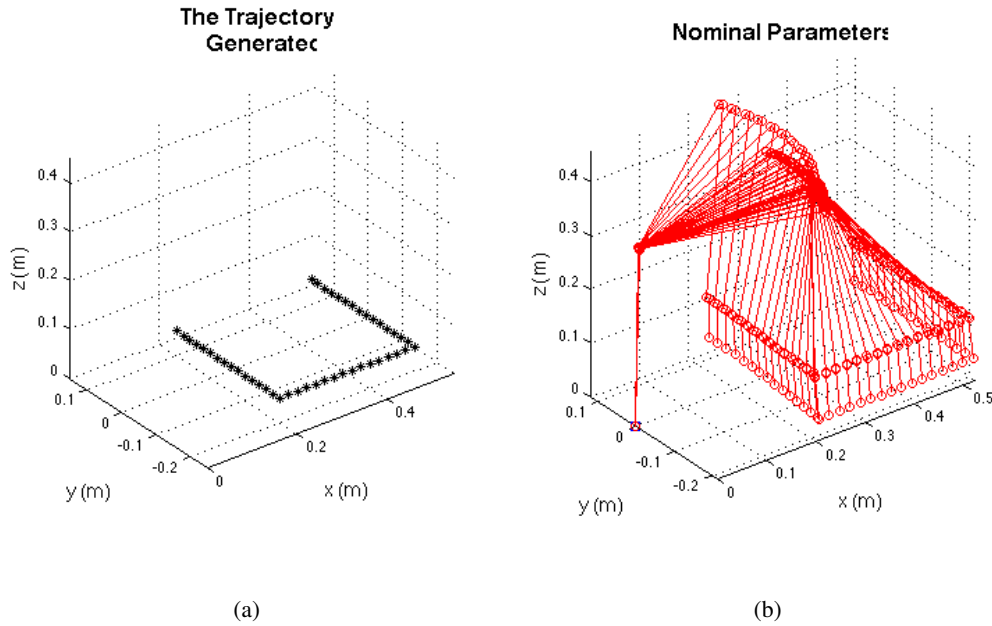


Fig. 6. The specified set of poses: (a) The end-effector coordinate system origin locations, and (b) The corresponding set of joint angles computed with the inverse kinematics.

The errors synthesized using Eq. (8) and (9) are stored in $\Delta\zeta$, and are added to the nominal DH parameter values. The trajectories i and j , which are based on Eqs. (3) and (6), are

$$\Delta\mathbf{x}_{rel} = \Delta\mathbf{x}_j^b - \Delta\mathbf{x}_i^b = (\mathbf{x}_{m,j}^b - \mathbf{x}_{n,j}^b) - (\mathbf{x}_{m,i}^b - \mathbf{x}_{n,i}^b), \quad (15)$$

where $\Delta\mathbf{x}_{rel} = [\Delta\mathbf{p}_{rel}, \Delta\Phi_{rel}]^T$.

The resulting Jacobian is used to obtain a first estimate of the synthesized errors, and the identified errors can be added to the nominal values to yield a new estimate of the DH parameters as

$$\zeta_{n,new} = \zeta_{n,old} + \Delta\zeta, \quad (16)$$

and the least-squares procedure is repeated until the convergence criterion is met, where $\Delta\zeta$ is below some specified threshold. For the experiments reported herein, the convergence criterion is defined using the

Euclidean 2-norm as [20]

$$\|\Delta\mathbf{x}_{rel} - \mathbf{J}_{rel}\Delta\zeta\|_2 \leq \varepsilon \text{rank}(\mathbf{V}), \quad (17)$$

where \mathbf{V} is an orthogonal matrix factor of the identification Jacobian obtained using a form of singular value decomposition (SVD), and ε is the machine's computational precision, which varies between the machine's CPU architecture. The identification Jacobian is additionally useful, because $\text{rank}(\mathbf{J}_{rel})$ indicates the number of parameters that can be identified.

3.1. Singular Value Decomposition (SVD)

Consider the linear system of equations in Eq. (13), where \mathbf{J}_{rel} is defined as the linear mapping from the vector space $\Delta\zeta$ to the vector space $\Delta\mathbf{x}_{rel}$. In order to estimate $\Delta\zeta$ in an overdetermined system of equations, one must understand how \mathbf{J}_{rel} maps the vector spaces. The *nullspace* of \mathbf{J}_{rel} maps the vector space $\Delta\zeta$ to $\mathbf{0}$, and the *range* of \mathbf{J}_{rel} maps the vector space $\Delta\zeta$ to $\Delta\mathbf{x}_{rel}$. The dimension of the nullspace and range of the matrix are referred to as the *nullity* and the *rank*, respectively. If \mathbf{J}_{rel} is nonsingular, then its range will consist of the entire vector space $\Delta\mathbf{x}_{rel}$, and its rank is N , indicating the matrix has a full-rank. If \mathbf{J}_{rel} is singular, the rank will be less than N , because some subspace of $\Delta\zeta$ is in the nullspace and what remains is in the range of \mathbf{J}_{rel} .

SVD decomposes the matrix of interest, \mathbf{J}_{rel} , into the product of three matrix factors:

$$(\mathbf{J}_{rel})_{M \times N} = (\mathbf{U}_{M \times M})(\mathbf{S}_{M \times N})(\mathbf{V}_{N \times N})^T, \quad (18)$$

where $\mathbf{S}_{M \times N}$ is an upper-diagonal matrix, whose elements on the diagonal consist the singular values, s_i , of \mathbf{J}_{rel} arranged in descending order; $\mathbf{U}_{M \times M}$ is a column-orthogonal matrix, whose same numbered elements s_i are nonzero are an orthonormal set of basis vectors that span the range; $\mathbf{V}_{N \times N}$ is an orthogonal matrix whose same numbered elements s_i are zero are an orthonormal basis for the nullspace.

Using SVD, the pseudo-inverse of the identification Jacobian can be computed as

$$(\mathbf{J}_{rel}^+)_{N \times M} = (\mathbf{V})_{N \times N}(\mathbf{S}^{-1})_{N \times M}(\mathbf{U}^T)_{M \times M}. \quad (19)$$

Since \mathbf{S} is an upper diagonal matrix consisting of singular values s_i , then \mathbf{S}^{-1} is also an upper diagonal matrix with elements $1/s_i$.

When the vector $\Delta\mathbf{x}$ is not $\mathbf{0}$, the vector may or may not lie in the range of \mathbf{J}_{rel} . If the vector $\Delta\mathbf{x}_{rel}$ lies in the range of \mathbf{J}_{rel} , then the singular matrix does have a solution $\Delta\zeta$, or possibly more than one solution, since any vector in the nullspace can be added to $\Delta\zeta$ in any linear combination. If the vector $\Delta\mathbf{x}_{rel}$ is not in the range of the singular matrix \mathbf{J}_{rel} , then Eq. (13) has no solution. While an exact solution for $\Delta\mathbf{x}_{rel}$ may not exist, an approximate solution can be constructed in a least-squares sense. In other words, the solution can be obtained by finding the set of $\Delta\zeta$ that minimizes the residual, r , of the solution:

$$r = \min \|\mathbf{J}_{rel}\Delta\zeta - \Delta\mathbf{x}_{rel}\|. \quad (20)$$

To approximate $\Delta\zeta$, in a least-squares sense using SVD, simply replace the reciprocals of singular values, $1/s_i$ by 0 if s_i is 0 or numerically close, where numerically close to zero refers to any floating point value less than, or equal to $\varepsilon \text{rank}(\mathbf{V})$. Finally compute

$$\Delta\zeta = \mathbf{V}\mathbf{S}^{-1}(\mathbf{U}^T\Delta\mathbf{x}_{rel}). \quad (21)$$

3.2. Simulation Results

Two simulations were performed to examine the performance of the algorithm. In the first only relative position measurements were simulated, while in the second relative orientation measurements were included.

3.2.1. Simulated Relative Position Measurements

In the first simulation, random noise is added to the nominal DH parameters, and the corresponding sets of joint angles were computed to follow the set of poses illustrated in Figure 6. Only relative position measurements were used and the simulation converged after the fourth iteration and a total CPU time of 0.57 seconds, reporting the residual:

$$\|\Delta \mathbf{x}_{rel} - \mathbf{J}_{rel} \Delta \zeta\|_2 \approx 1.1899 \times 10^{-15}.$$

The convergence threshold was set to $\epsilon \text{rank}(\mathbf{V}) \approx 5.3291 \times 10^{-15}$, where $\text{rank}(\mathbf{V}) = 24$ and $\epsilon \approx 2.2204 \times 10^{-16}$ on the computer used.

| | Joint Errors [deg] | | | | | | Link Errors [mm] | | | | | |
|--------|----------------------|----------------------|-------|----------------------|----------------------|--------|------------------|-----------------|-------|-----------------|-----------------|-------|
| | $\Delta \theta_{sp}$ | $\Delta \theta_{id}$ | % | $\Delta \alpha_{sp}$ | $\Delta \alpha_{id}$ | % | Δa_{sp} | Δa_{id} | % | Δd_{sp} | Δd_{id} | % |
| 1 | 0.175 | 0.175 | 0.000 | -0.789 | -0.789 | 0.000 | 0.891 | 0.891 | 0.000 | 0.367 | 0.000 | 100.0 |
| 2 | -0.150 | -0.150 | 0.000 | 0.254 | 0.254 | 0.000 | 0.253 | 0.253 | 0.000 | -0.093 | -0.093 | 0.000 |
| 3 | 0.011 | 0.011 | 0.000 | 0.141 | 0.141 | 0.000 | 0.422 | 0.422 | 0.000 | 0.235 | 0.235 | 0.000 |
| 4 | -0.131 | -0.131 | 0.000 | 0.017 | 0.017 | 0.000 | -0.324 | -0.324 | 0.000 | -0.686 | -0.686 | 0.000 |
| 5 | -0.875 | -0.875 | 0.000 | -0.667 | -0.667 | 0.000 | -0.144 | -0.144 | 0.000 | -0.118 | -0.118 | 0.000 |
| 6 | -0.143 | -0.143 | 0.000 | 0.564 | 0.000 | 100.0 | -0.083 | -0.083 | 0.000 | -0.275 | -0.275 | 0.000 |
| RMS | | | | | | | | | | | | |
| 0.0040 | | | | | | 0.0001 | | | | | | |

Table 2. Simulation results of the kinematic calibration using relative position measurements.

Table 2 lists the identification results for the first simulation, along with the percent errors relative to the specified parameter error values for the relative position measurements. The root mean square (RMS) errors in the identified parameters from the specified parameter errors are also listed, and these results are a measure of the accuracy of the identification. The simulation consists only of relative position error, and $\text{rank}(\mathbf{J}_{rel}) = 22$, which means that there are 2 of the 24 parameter errors were not observable, while 22 were identified correctly. As shown in Table 2, the two parameters that cannot be identified are Δd_1 and $\Delta \alpha_6$. Because the relative position measurement concept does not account for the absolute location of the manipulator base coordinate system origin, Δd_1 cannot be identified. Moreover, $\Delta \alpha_6$ is unobservable because of the absence of orientation measurements about the end-effector joint axis.

3.2.2. Simulated Relative Orientation Measurements

In the second simulation using relative pose measurements, the algorithm converged after the sixth iteration and the total CPU time of 1.14 seconds with the following residual:

$$\|\Delta \mathbf{x}_{rel} - \mathbf{J}_{rel} \Delta \zeta\|_2 \approx 3.6549 \times 10^{-15}.$$

However, once additional random noise was added to the nominal DH parameters, the simulation converged after the fourth iteration and a total CPU time of 0.63 seconds, reporting a residual of

$$\|\Delta \mathbf{x}_{rel} - \mathbf{J}_{rel} \Delta \zeta\|_2 \approx 3.8803 \times 10^{-15}.$$

Table 3 summarizes the results. The simulation incorporated both the relative position and orientation error measurements. The corresponding identification Jacobian possessed $\text{rank}(\mathbf{J}_{rel}) = 23$. This means that 23 of the 24 parameters were identified correctly. In this case, Δd_1 still cannot be identified because information regarding the base frame origin is lost in the subtraction leading to the relative pose errors.

| | Joint Errors [deg] | | | | | | Link Errors [mm] | | | | | |
|-----|---------------------|---------------------|--------|---------------------|---------------------|--------|------------------|-----------------|-------|-----------------|-----------------|-------|
| | $\Delta\theta_{sp}$ | $\Delta\theta_{id}$ | % | $\Delta\alpha_{sp}$ | $\Delta\alpha_{id}$ | % | Δa_{sp} | Δa_{id} | % | Δd_{sp} | Δd_{id} | % |
| 1 | 0.175 | 0.175 | 0.000 | -0.789 | -0.789 | 0.000 | 0.891 | 0.891 | 0.000 | 0.367 | 0.000 | 100.0 |
| 2 | -0.150 | -0.150 | 0.000 | 0.254 | 0.254 | 0.000 | 0.253 | 0.253 | 0.000 | -0.093 | -0.093 | 0.000 |
| 3 | 0.011 | 0.011 | 0.000 | 0.141 | 0.141 | 0.000 | 0.422 | 0.422 | 0.000 | 0.235 | 0.235 | 0.000 |
| 4 | -0.131 | -0.131 | 0.000 | 0.017 | 0.017 | 0.000 | -0.324 | -0.324 | 0.000 | -0.686 | -0.686 | 0.000 |
| 5 | -0.875 | -0.875 | 0.000 | -0.667 | -0.667 | 0.000 | -0.144 | -0.144 | 0.000 | -0.118 | -0.118 | 0.000 |
| 6 | -0.143 | -0.143 | 0.000 | 0.564 | 0.564 | 0.000 | -0.083 | -0.083 | 0.000 | -0.275 | -0.275 | 0.000 |
| RMS | | | 0.0000 | | | 0.0001 | | | | | | |

Table 3. Simulation results incorporating relative orientation measurement.

4. CONCLUSIONS

The relative measurement based calibration method presented in this paper identifies 23 out of 24 modelled kinematic parameters. The lone unidentified parameter is an artifact of the non-observability of the manipulator base coordinates. Absolute measurements are required to identify the final parameter correctly, which requires expensive equipment to measure the absolute geometry with high precision. Despite the unobservability of only one parameter, the relative measurement method leads to a low-cost system constructed with readily available off-the-shelf items such as a high-resolution camera and a laser printed chess grid mounted to a plate that is capable of improving a six axis serial robot arms accuracy up to the same order of magnitude as the manipulators repeatability. Furthermore, it is straightforward to implement in a working production cell, or on the manufacturing floor. Moreover, it can easily be applied to any serial manipulator.

REFERENCES

1. Z. Roth, B. Mooring, and B. Ravani. "An Overview of Robot Calibration," *IEEE Trans. Robotics Automat.*, vol.3 pp. 377–386, 1987.
2. Morris R. Driels, and William E. Swayze. Automated Partial Pose Measurement System for Manipulator Calibration Experiments. *IEEE Transaction on Robotics and Automation*, VOL. 10, NO. 4, 1994.
3. Benjamin W. Mooring, Zvi S. Roth, and Morris R. Driels. *Fundamentals of Manipulator Calibration*. John Wiley Sons, Inc., 1991.
4. J.Chen and L. Chao, "Positioning Error Analysis for Robot Manipulator with All Rotary Joints," *In Proc. 1986 IEEE International Conference on Robotics and Automation*. April 1986, pp. 1011–1016.
5. Robert P. Judd and Al B. Knasinski, A technique to calibrate industrial robots with experimental verification. In *Proceeding of 1987 IEEE International Conference on Robotics and Automation*, pp. 351-357, April 1987.
6. L.J. Everett, Morris Driels, and B.W. Mooring. Kinematic modelling for robot calibration. In *Proceedings of the 1987 IEEE International Conference on Robotics and Automation*, pp. 183-189, April 1987.
7. C. H. Wu. "A Kinematic CAD Tool for the Design and Control of a Robot Manipulator", *The International Journal of Robotics Research*, 3(1), pp. 58-67, 1984.
8. H. S. Lee, S.L. Chang. Development of a CAD/CAE/CAM System for a Robot Manipulator. *The Journal of Materials Processing Technology*, pp. 100-104, 2003.
9. I-Ming Chen, Guilin Yang, Chee Tat Tan, and Song Huat Yeo. Local POE model for Robot Kinematic Calibration. *Mechanism and Machine Theory*, pp. 1215-1239, 2001.
10. Yunjiang Lou, Tieniu Chen, Yuanqing Wu, and Guanfeng Liu. Computer Vision Based Calibration of the Purely Translational Orthopod Manipulator. *Proceedings of the 2009 IEEE International Conference on Information*

- and Automation*, June 2009.
11. Yan Meng, and Hanqi Zhuang. Self-Calibration of Camera-Equipped Robot Manipulators. *The International Journal of Robotics Research*, November 2001.
 12. In-Won Park, Bum-Joo Lee, Se-Hyoung, Young-Dae Hong, and Jong-Hwan Kim. Laser-Based Kinematic Calibration of Robot Manipulator Using Differential Kinematics. *IEEE/ASME Transactions on Mechatronics*, 2012.
 13. Hanqi Zhuang, Wen-Chiang Wu, and Zvi S. Roth. Camera-Assisted Calibration of SCARA Arms. *Proceedings IEEE/RSJ International Conference on Intelligent Robots and Systems, Human Robot Interaction and Cooperative Robotics*, 1995.
 14. H. Hage, P. Bidaud, and N. Jardin, Practical Consideration on the Identification of the Kinematic Parameters of the Staübli TX90 Robot. *13th World Congress in Mechanism and Machine Science*, Guanajuato, Mexico, 2011.
 15. Dali Wang, Ying Bai, and Jiying Zhao. Robot Manipulator Calibration using Neural Network and a Camera-Based Measurement System. *Transactions of the Institute of Measurement and Control*, 2010.
 16. N.W. Simpson, M.J.D. Hayes, Simulation of a Kinematic Calibration Procedure that Employs the Relative Measurement Concept, *Proceedings of the CSME Forum 2004*, University of Western Ontario, London, ON, Canada, pp. 62-71, June 1-4, 2004.
 17. A.A. Fratpietro, M.J.D. Hayes, Relative Measurement for Kinematic Calibration Using Digital Image Processing, *Proceedings of the CSME Forum 2004*, University of Western Ontario, London, ON, Canada, pp. 758-767, June 1-4, 2004.
 18. In-Chul, Ha, *Kinematic parameter calibration method for industrial robot manipulator using the relative position*, Institute of Industrial Technology 103-28, Mounji-dong, Yuseong-gu, Daejeon 305-380, Korea, 2008.
 19. Denavit, J., Hartenberg, R.S., "A Kinematic Notation for Lower-Pair Mechanisms Based on Matrices", *J. of Applied Mechanics*, pp. 215-221, 1955.
 20. William H. Press, Saul A. Teukolsky, William T. Vetterling, and Brian P. Flannery. *Numerical Recipes in C: The Art of Scientific Computing*. Cambridge University Press, 2nd edition, 1992.